AGU PUBLICATIONS

JGR

Journal of Geophysical Research: Space Physics

TECHNICAL REPORTS: DATA

10.1002/2015JA021808

Key Points:
- Thermospheric Na layers extending up to 170 km observed for the first time at Lijiang, China
- Thermospheric Na layers descend at 11-12 km/h consistent with semidiurnal tidal phase speed
- Observational evidence of correlation between thermosphere Na layers and equatorial fountain effect

Correspondence to:
X. Chu and X. Dou,
Xinzhao.Chu@colorado.edu;
dou@ustc.edu.cn

Citation:
Gao, Q., X. Chu, X. Xue, X. Dou, T. Chen, and J. Chen (2015), Lidar observations of thermospheric Na layers up to 170 km with a descending tidal phase at Lijiang (26.7°N, 100.0°E), China, *J. Geophys. Res. Space Physics*, *120*, 9213–9220, doi:10.1002/2015JA021808.

Received 13 AUG 2015
Accepted 1 OCT 2015
Accepted article online 5 OCT 2015
Published online 27 OCT 2015

Lidar observations of thermospheric Na layers up to 170 km with a descending tidal phase at Lijiang (26.7°N, 100.0°E), China

Qi Gao[1,2], Xinzhao Chu[2], Xianghui Xue[1,3,4], Xiankang Dou[1,3], Tingdi Chen[1,3], and Jinsong Chen[5,6]

[1]CAS Key Laboratory of Geospace Environment, Department of Geophysics and Planetary Sciences, University of Science and Technology of China, Hefei, China, [2]Cooperative Institute for Research in Environmental Sciences and Department of Aerospace Engineering Sciences, University of Colorado Boulder, Boulder, Colorado, USA, [3]Mengcheng National Geophysical Observatory, School of Earth and Space Sciences, University of Science and Technology of China, Hefei, China, [4]Synergetic Innovation Center of Quantum Information and Quantum Physics, University of Science and Technology of China, Hefei, China, [5]National Key Laboratory of Electromagnetic Environment, China Research Institute of Radiowave Propagation, Qingdao, China, [6]State Key Laboratory of Space Weather, Chinese Academy of Sciences, Beijing, China

Abstract We report the first lidar observations of thermospheric Na layers up to 170 km at Lijiang (geomagnetic 21.6°N, 171.8°E), China, in March, April, and December 2012. The Na densities inside the layers are low, ranging from ~1 to ~6 cm^{-3} at altitudes of 130–170 km, about 3 orders of magnitude lower than the Na peak density in the mesopause region. All of these layers exhibit an apparent downward phase progression with a descending rate of 11–12 km/h or ~3 m/s, consistent with the vertical phase speed of semidiurnal tides around 140 km. We have identified at least 12 events from the total 37 nights of lidar observations with four shown in this report, giving an occurrence frequency of ~33% over Lijiang. These thermospheric layer events correspond to strong to moderate equatorial fountain effects, bolstering our hypothesis that the deposit of metallic ions from the equatorial region to low latitudes via the fountain effect provides the Na^+ ions in the thermosphere over Lijiang. Adopting the theory by Chu et al. (2011) and the hypothesis by Tsuda et al. (2015), we further hypothesize that the thermospheric Na layers are formed through the neutralization of the tidal-wind-shear-converged Na^+ layers via direct electron-Na^+ recombination $Na^+ + e^- \rightarrow Na + h\nu$. An envelope calculation using reasonable ion and electron densities shows good consistency with the observations.

1. Introduction

The neutral metal atom layers (e.g., Fe, Na, and K) are normally confined to altitudes of 75–110 km, as many lidar observations have shown (see summaries in *Plane* [2003] and *Chu and Papen* [2005]), though the natural extension of the main layers has been detected up to 130 km with highly sensitive lidars [*Höffner and Friedman*, 2004, 2005]. New discoveries in recent years have radically changed our view on the range limit of neutral metal layers. *Chu et al*. [2011] reported the first lidar observations of neutral Fe layers with gravity wave signatures in the thermosphere up to 155 km at McMurdo (77.83°S, 166.66°E), Antarctica. *Lübken et al*. [2011] observed Fe layers to at least 140 km at Davis (69°S, 78°E), Antarctica. Continuous Fe lidar observations at McMurdo have revealed thermospheric Fe layers exceeding 170 km [*Chu et al*., 2013, 2015]. Using these layers as tracers, *Chu et al*. [2011, 2013] were able to derive neutral atmosphere temperatures from ~30 to ~170 km by combining the Fe Boltzmann technique with the Rayleigh integration technique [*Gelbwachs*, 1994; *Chu et al*., 2002]. Checking historic data, *Friedman et al*. [2013] reported a descending K layer up to ~155 km in the thermosphere, occurring on 12 March 2005 at Arecibo, Puerto Rico (18.35°N, 66.75°W), while *Tsuda et al*. [2015] reported Na layers up to 140 km occurring on 23–24 September 2000 at Syowa (69.0°S, 39.6°E), Antarctica. *Wang et al*. [2012] presented descending Na layers with high densities in the lower thermosphere below 130 km over Beijing (40.2°N, 116.2°E), and *Xue et al*. [2013] reported two enhanced Na layers below 130 km for Lijiang (26.7°N, 100.0°E). *Dou et al*. [2013] conducted a statistical study of enhanced Na layers with a lidar chain at Beijing, Hefei (31.8°N, 117.3°E), Wuhan (30.5°N, 114.4°E), and Haikou (19.5°N, 109.1°E) in China.

As of the end of year 2013, Na layers have not been reported above 140 km, well below the records for Fe and K layers. This situation raises interesting questions. Are the unusually high Fe layers observed unique to McMurdo or a property of Fe itself? Can other species, like Na, occur above 140 km at locations other than Antarctica? These questions are important because the answers to them will provide useful insight into

the origin of these neutral metal layers and their formation mechanisms. According to the theory originally proposed by *Chu et al*. [2011] and later modeling studied by *Yu and Chu* [2014], the observed neutral Fe layers are formed through the neutralization of vertically converged Fe^+ ion layers, and the main neutralization channel is the direct electron-Fe^+ recombination: $Fe^+ + e^- \rightarrow Fe + h\nu$. As Fe^+, Na^+, and K^+ all have been detected in ion layers [*Kopp*, 1997; *Roddy et al*., 2004], converged Na^+ and K^+ layers are expected to accompany converged Fe^+ layers. Consequently, neutral Na and K layers are expected to occur as high as Fe layers via similar direct electron-ion recombination [*Friedman et al*., 2013; *Tsuda et al*., 2015]. However, because Na^+ density is usually much lower than Fe^+ in the lower ionosphere [*Kopp*, 1997], it is likely that the Na density is much less than Fe in the thermosphere. Consequently, very high detection sensitivity is required on Na lidars for detection of such tenuous layers.

This study aims at providing one of the first answers to the above questions with the Na lidar data collected from Lijiang (26.7°N, 100.0°E), China, where a large-aperture astronomical telescope [*Wei et al*., 2010] helped improve the lidar detection sensitivity, thereby enabling the detection of weak Na layers at this site. *Xue et al*. [2013] reported Na layers at Lijiang up to 122 km, as mentioned above. After reprocessing the data following the method given in *Chu et al*. [2011], we have discovered thermospheric Na layers up to 170 km on at least four days in March, April, and December 2012 at Lijiang. In this paper we report these first (to our knowledge) observations of thermospheric Na layers up to 170 km. It is worth mentioning that following the Lijiang observations, neutral Na layers were observed up to 170 km in May 2014 and the following months at Cerro Pachón, Chile, after a lidar team from the University of Colorado upgraded the University of Illinois Na Doppler lidar and significantly improved its detection sensitivity [*Smith and Chu*, 2015]. Although it is still too early to "paint" a global picture of the occurrence and distribution of thermosphere neutral metal layers, we will demonstrate in this study that thermospheric Fe species are not unique to McMurdo, and that we expect other metal layers, like Na and K, to occur high into the thermosphere at other locations on Earth.

2. Observations

The lidar observations were made at Gaomeigu Astronomical Observatory in Lijiang, China, with a broadband dye-laser-based Na resonance fluorescence lidar developed by the University of Science and Technology of China [*Xue et al*., 2013]. The observational campaigns were first conducted from 8 March to 15 April 2012 and then again from 27 November to 15 December 2012. A total of 37 nights of lidar data were obtained. Several factors enabled the high detection sensitivity of this lidar: the 1.8 m diameter Cassegrain telescope [*Wei et al*., 2010] implemented in the lidar receiver, the high base elevation of 3.3 km, and the clear skies for astronomical observations at this site. In order to further improve the detection limit and enhance the visibility of tenuous layers, the raw data, with resolutions of 25–50 s and 96 m, are smoothed using Hamming windows with a full width at half maximum of 7.5 min and 0.9 km, then oversampled at steps of 1 min and 96 m, following the oversampling method used in *Chu et al*. [2011]. This method improves the signal-to-noise ratio while retaining high display resolutions without any interpolation. Such high-resolution density contours are important to identify tenuous metal layers with a downward phase progression from background noise, as demonstrated in *Chu et al*. [2011], *Friedman et al*. [2013], and *Tsuda et al*. [2015].

Illustrated in Figure 1 are four cases of neutral Na layers extending well into the thermosphere on 11 and 31 March 2012, 10 April 2012, and 3 December 2012 at Lijiang. While the main Na layers are located between ~80 and ~110 km, the descending Na layer, with an obvious downward phase progression, is distinct from the main layer above 120 km and extended to ~170 km on every night. These thermospheric Na layers are very tenuous—nearly 3 orders of magnitude less dense than the peak of the main layer. Figure 2 shows the Na density profiles for comparison. The strongest layer occurred on 10 April 2012, with the maximum Na density of ~6.3 cm^{-3} occurring at 138 km, falling to ~1.8 cm^{-3} at 170 km. In the other three cases, the thermospheric Na densities are generally ~3 cm^{-3} or lower and drop to ~1 cm^{-3} near the layer top (~160–170 km). Such low densities are usually undetectable. Fortunately, the detection limit of the Na lidar used in this study was well below 1 cm^{-3}, as indicated by the vertical dashed lines in Figure 2, making the detection of such tenuous layers possible. Because the Na layer densities are well above the detection limit and, more importantly, the Na layers exhibit apparent downward phase progressions (Figure 1), the detection of thermospheric Na layers to 170 km at Lijiang is unequivocal.

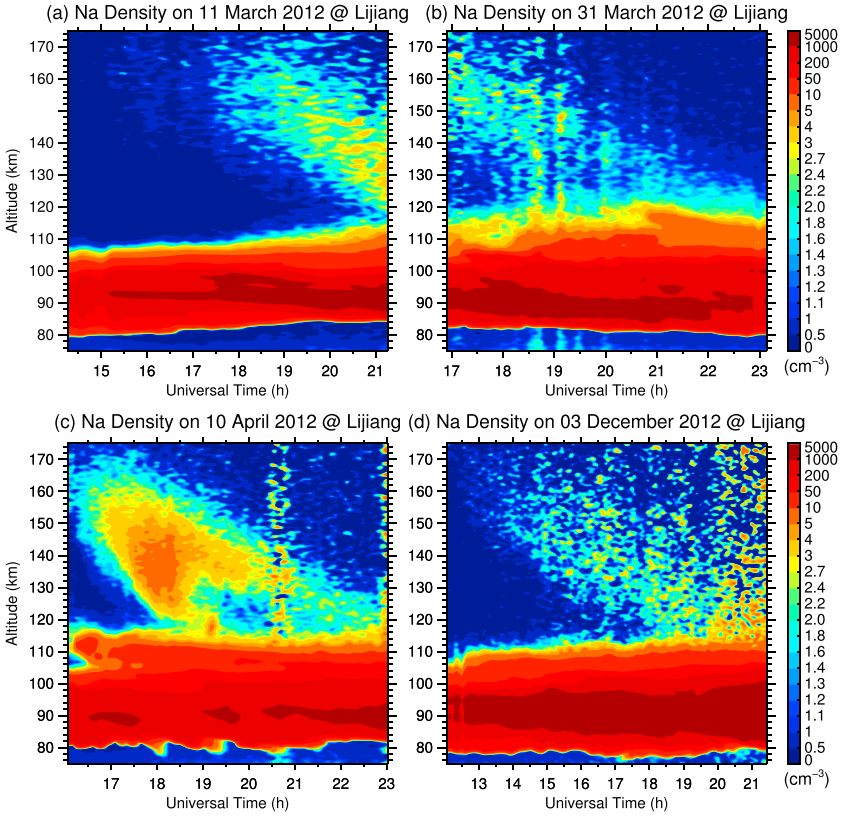

Figure 1. Thermospheric Na layers up to 170 km observed by lidar respectively on 11 March, 31 March, 10 April, and 3 December 2012 at Lijiang, China. Note that the color scales are unequally spaced.

The thermospheric Na densities are strikingly low at Lijiang. Even the strongest layer on 10 April 2012 is about 10 times lower than the thermospheric Fe layer densities (~20–200 cm^{-3}) reported by *Chu et al*. [2011] for May 2011 at McMurdo. The Na densities are comparable to the Na event at Syowa [*Tsuda et al*., 2015] but higher than the thermospheric K layer densities ($<$1 cm^{-3}) at Arecibo [*Friedman et al*., 2013]. Another interesting feature is the long layer duration and large vertical extent. Taking 140 km on 10 April as an example, the thermospheric Na layer lasts ~4 h, edge to edge, much longer than the Fe and Na layers observed at McMurdo and Syowa and also longer than the Arecibo K layer duration. The Na layer profiles span ~30–40 km in altitude (Figure 2), comparable to the other three sites.

In stark contrast to the repeated occurrence of Fe layers with periods of 1.5–3 h at McMurdo [*Chu et al*., 2011, 2013], the Na layer only appears once per night at Lijiang. The descending rate V_z is roughly estimated by a linear fit to the Na layer of 120–170 km on 10 April. The estimated V_z is ~11–12 km/h or ~3 m/s, much slower than the gravity-wave-driven thermospheric Fe layers at McMurdo but comparable to the ~9.2 km/h descending rate of the Arecibo K layer. Following *Friedman et al*. [2013], we utilize the Global-Scale Wave Model (GSWM-09) to investigate whether the descending rate matches any of the tidal components at Lijiang. GSWM-09 is an upgraded version of the Global-Scale Wave Model [*Hagan and Forbes*, 2002, 2003], which includes updated, more realistic background winds and temperatures and radiative and latent heating rates [*Zhang et al*., 2010a, 2010b]. In this study, the diurnal and semidiurnal tides retrieved from GSWM-09 include both migrating and nonmigrating components with wavenumbers from −6 to +6. The temperature tidal amplitudes and phases are shown in Figure 3 for March, April, and December at Lijiang. According to the model, semidiurnal tides dominate over diurnal tides in amplitudes above 115 km. The phase speeds of the semidiurnal tides are ~10 km/h from 120 to 145 km and increase to ~20 km/h by 160 km. The average phase speed between 120 and 160 km is comparable to the measured descending rate of the thermospheric Na layers. Plotting the cold and hot phases of the diurnal and semidiurnal tides over the Na density contours in the bottom row of Figure 3, we find that the cold phase of the semidiurnal tides closely matches the Na layer crests on

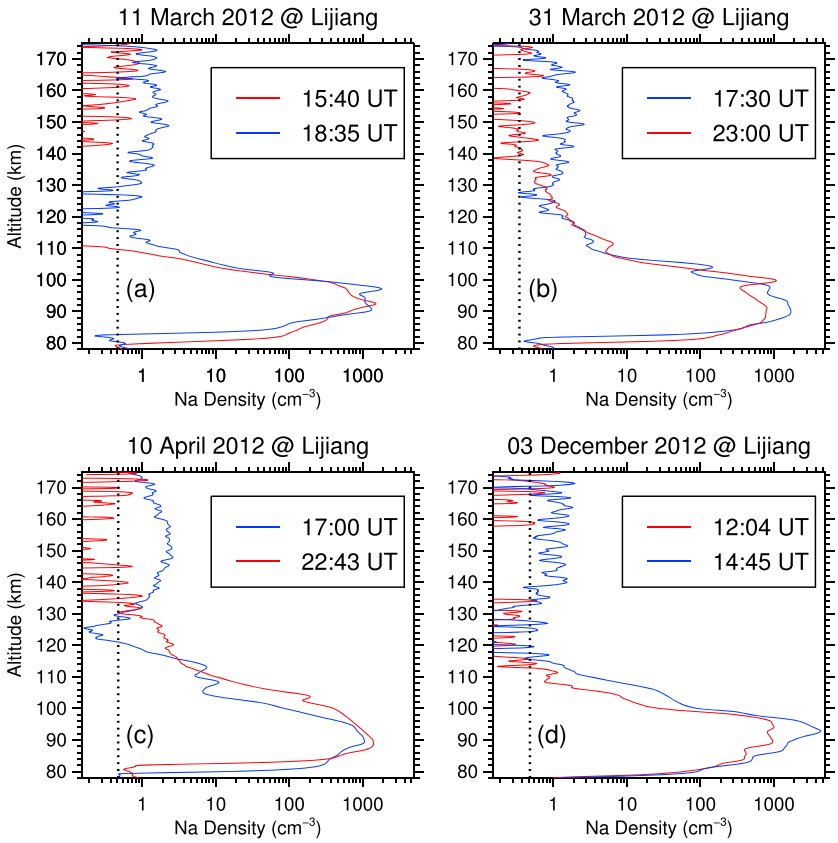

Figure 2. The vertical profiles of Na densities for the four cases in Figure 1. The blue and red lines represent the profiles with and without thermospheric Na layers, respectively, at the given times. The black lines denote the lidar detection limits that are given by 1.5 times of the standard deviation of the background photon noise.

10 April and 31 March, while the hot phase matches the crest on 3 December well. For the case on 11 March, the cold phase and the Na crest are consistent in shape but exhibit a ~2 h time shift. The nearly perfect match of semidiurnal tidal phase lines with the observed Na layers strongly suggests that the thermospheric Na layers at Lijiang are driven by semidiurnal tides, consistent with the Arecibo finding [*Friedman et al.*, 2013].

Despite the large differences in characteristics between Lijiang's Na and McMurdo's Fe layers, the contrast of the thermospheric Na layers at Lijiang is significant—regions without Na (e.g., above the main layer but below the thermospheric layer) are clearly distinguished from the thermospheric layers, resembling the high contrast of thermospheric Fe layers at McMurdo. As argued by *Chu et al.* [2011] and supported by modeling in *Yu and Chu* [2014], such high contrast cannot be obtained by wave perturbation to the neutral atmosphere but must result from ion layers that are converged and then neutralized to form detectable, neutral metal layers [*Yu*, 2014]. Therefore, we investigate the ionospheric conditions. Plotted in Figure 4 are two sets of data: the vertical total electron content (TEC) distribution derived from ground-based GPS measurements (http://iono.jpl.nasa.gov/latest_rti_global.html) and the ionosonde data from Kunming Radio Observatory (25.6°N, 103.8°E), a station 300 km away from Lijiang. The features of a deep trough at the magnetic equator and two peaks at about ±15° off the equator in the TEC distribution (Figure 4) are the well-known equatorial anomaly phenomenon or the equatorial fountain effect. The fountain effect uplifts ions and electrons from the magnetic equator and then redistributes them along the magnetic field lines to two sides [e.g., *Pi et al.*, 2009]. Consequently, the partial depletion over the magnetic equator forms a trough and the accumulation of the plasma off the equator forms a peak on each side. Lijiang experiences strong fountain effects on the four days of thermospheric layer events.

Among the 37 nights of lidar observations at Lijiang, we have found at least eight more events of thermospheric Na layers reaching 140–160 km. Although their densities are even lower than the four cases investigated here, they all exhibit clear downward phase progressions with high contrasts. Therefore, we can estimate the

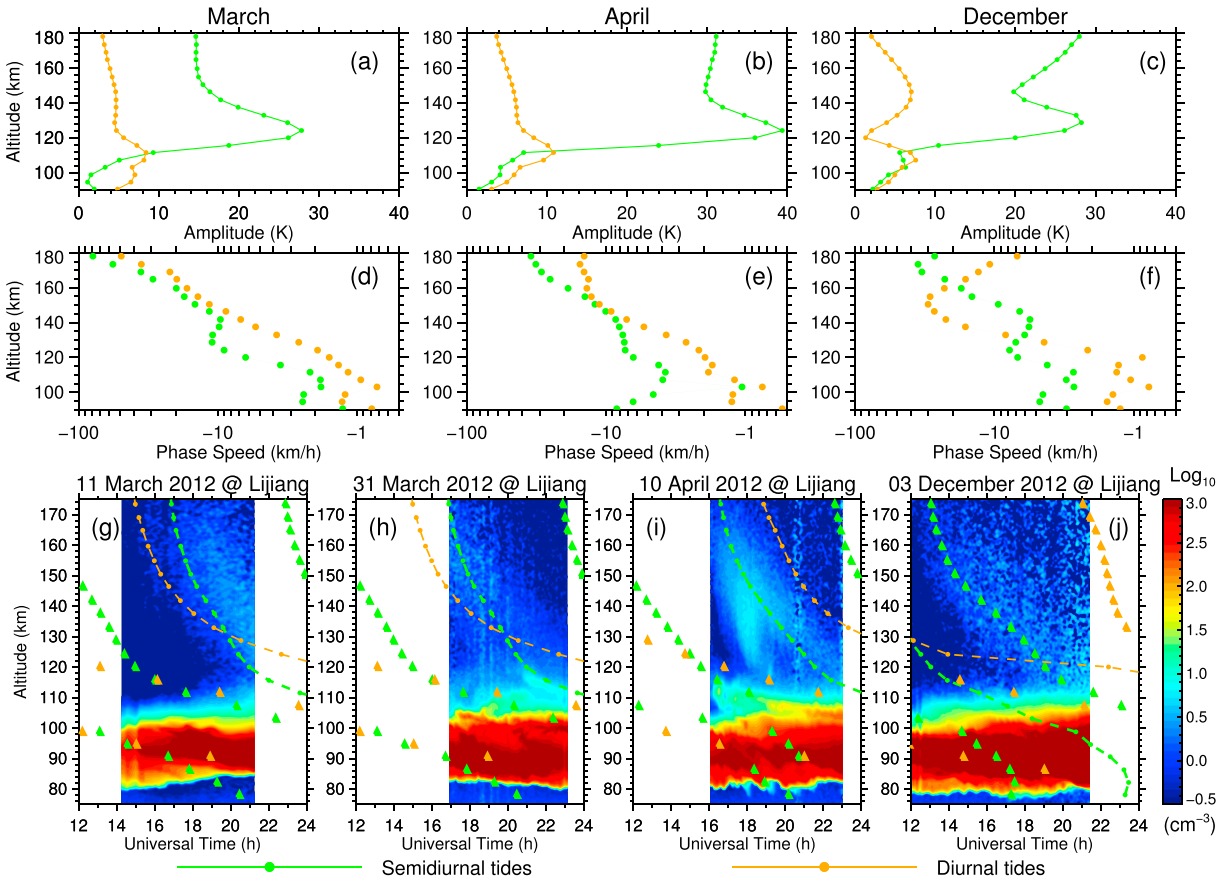

Figure 3. GSWM-09 simulated diurnal and semidiurnal temperature tides: (top row) Amplitudes and (middle row) vertical phase speeds in March, April, and December. (bottom row) GSWM-09 temperature tidal phases overplotted on the Na density contours for the four cases in Figure 1. Orange and green colors denote diurnal and semidiurnal tides, respectively, while triangles and dashed lines represent, respectively, the hot and cold phases of the temperature tides.

occurrence frequency of thermospheric Na layers above Lijiang at ~33%. Interestingly, all of these 12 cases correspond to strong to moderate equatorial fountain effects indicated by the magnitudes of two peaks in the TEC distribution.

3. Discussion

The observed high contrast hints at a metallic ion origin of neutral metal layers in the thermosphere. Guided with the latest understandings gained from recent work by *Chu et al.* [2011, 2015] and *Yu and Chu* [2014], we propose the following explanation for the formation of thermospheric neutral metal layers over Lijiang. Three major steps are involved according to *Yu and Chu* [2014] and *Chu et al.* [2015]: (1) the transport of metallic ions and electrons from their main deposition regions below 120 km to the *E* and *F* regions; (2) convergence of these metallic ions, e.g., by wind shear mechanisms, to form dense ion layers in the thermosphere; and (3) neutralization of the metallic ions (Fe^+, Na^+, and K^+) through direct electron-ion recombination to form neutral metal layers (Fe, Na, and K). The polar electric field provides the necessary upward transport of ions in the polar region as modeled by *Yu and Chu* [2014], while the equatorial fountain effect plays a vital role in transporting ions at low latitudes as modeled by e.g., *Carter and Forbes* [1999] and *Bishop and Earle* [2003]. The $\vec{E} \times \vec{B}$ plasma drift uplifts ions in the equatorial region to sufficiently high altitudes (e.g., several hundreds of kilometers to even 1000 km), and then gravity and diffusion redistribute ions along the geomagnetic field lines (in the meridional plane) poleward and downward. Such upward plasma drift usually peaks in the early afternoon, but it takes several to many hours for the uplifted ions to redistribute to lower *F* region and *E* region at low latitudes. This fountain effect results in a significant ion density enhancement in the *F* region including F_1 layer (around 200 km) in the evening and nighttime at low-latitude sites such as Lijiang

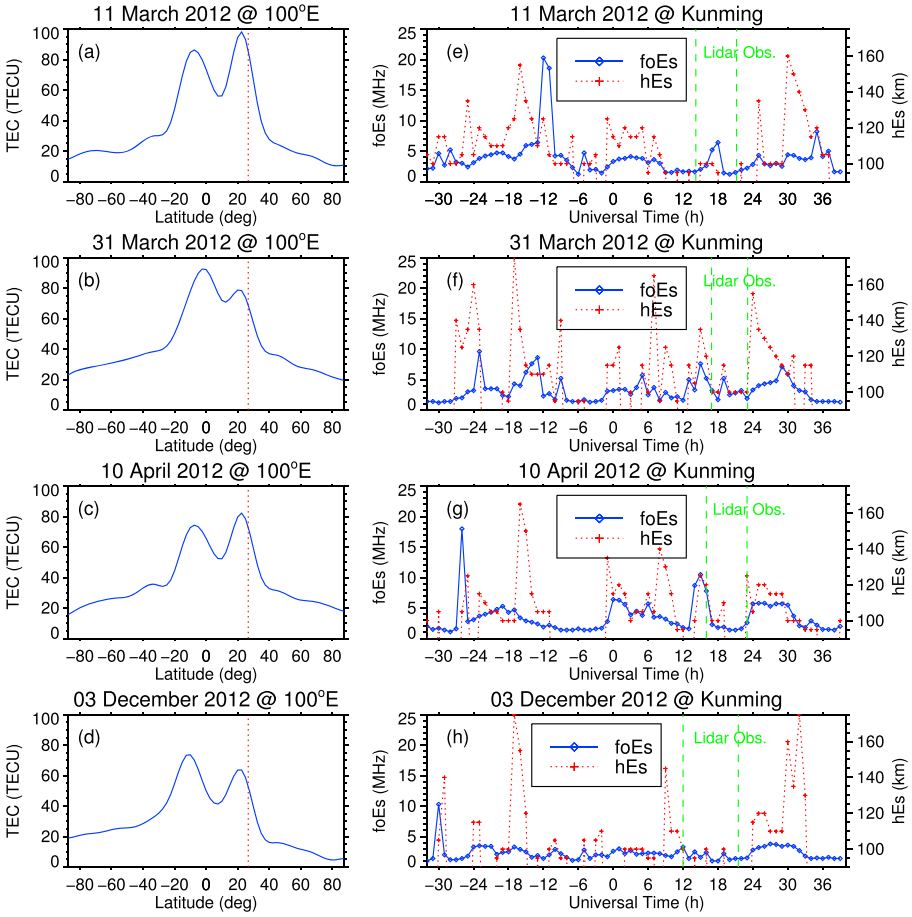

Figure 4. (left column) The TEC profiles at the longitude of Lijiang (100°E) averaged over 6–10 UT when the TEC reaches the maximum. The red dashed lines indicate the latitude of Lijiang. (right column) The critical frequency f_oE_s and virtual height hE_s of sporadic *E* layers observed by an ionosonde at Kunming. The lidar observational periods are marked by green dashed lines.

(geomagnetic: 21.6°N, 171.8°E), thus providing the sources of Na^+ to "seed" the neutral layer formation. The observed correlation between the thermospheric Na layers and the equatorial fountain effects supports this hypothesis.

Converged ion layers are required in the current explanation because of the very low reaction rate coefficients for $Na^+ + e^- \rightarrow Na + h\nu$. The densities of Na^+ and electrons must be high enough for the Na production rate to exceed the loss rate from charge transfer and other loss mechanisms. Diffusively distributed Na^+ ions will not have the needed density; therefore, Na^+ must be converged to form dense layers. Although dissociative recombination was found to be responsible for the sporadic Na layers below 110 km [*Cox and Plane*, 1998; *Collins et al.*, 2002; *Plane*, 2003], it would not be effective above 120 km due to the low atmospheric density. The only known path to convert Na^+ to Na at high altitudes is the direct (radiative) recombination $Na^+ + e^- \rightarrow Na + h\nu$ [*Plane et al.*, 2015]. Though this reaction is very slow, it is still possible to form thermospheric Na layers, as shown below following a similar envelope calculation as *Chu et al.* [2011]. In a night when photoionization of Na is absent, the loss of Na is mainly through charge transfer $Na + NO^+ \rightarrow Na^+ + NO$ and $Na + O_2^+ \rightarrow Na^+ + O_2$, with reaction rate coefficients of $8.0 \times 10^{-10} cm^3 s^{-1}$ and $2.7 \times 10^{-9} cm^3 s^{-1}$, respectively [*Daire et al.*, 2002]. It is reasonable to assume that the total density of NO^+ and O_2^+ is less than $1 \times 10^4 cm^{-3}$ [*Chu et al.*, 2011]. Then the loss rate of Na by charge transfer is $\sim 3.5 \times 10^{-5} s^{-1}$, giving a nighttime Na lifetime of ~8 h consistent with the estimate by *Plane et al.* [2015]. Regarding Na production, we inspect a sporadic *E* layer that occurred on 10 April 2012, before the thermospheric Na layer (Figure 4). The critical frequency f_o of the layer was ~7.8 MHz at 16 UT with a virtual height of 120 km, so an electron density $N_e = 1.24 \times 10^4 f_o^2 = 7.5 \times 10^5 cm^{-3}$ is

estimated. Consequently, we assume $N_e \sim 10^5 \mathrm{cm}^{-3}$ at higher altitudes. The reaction rate coefficient for $Na^+ + e^- \rightarrow Na + h\nu$, at 500 K that is typical for the thermosphere, is $k = 1.98 \times 10^{-12} \mathrm{cm}^3 \mathrm{s}^{-1}$ [*Plane et al.*, 2015; *Verner and Ferland*, 1996]. To produce a Na density of ~6 cm^{-3} within 2 h, $[Na^+] \approx 4.4 \times 10^3 \mathrm{cm}^{-3}$ is needed, occupying ~4.4% of the total ions if it is assumed equal to the electron density. This result is reasonable and in agreement with rocket measurements by *Kopp* [1997].

Wind shear mechanisms [e.g., *Whitehead*, 1961] readily provide the necessary vertical ion convergence at Lijiang, not only forming dense Na^+ layers but also increasing the electron density to expedite neutralization. The cold phases of semidiurnal tides in the first three cases of Figure 3 accelerate the conversion from Na^+ to Na due to the higher recombination rate at lower temperatures, while the hot phase on 3 December 2012 slows down the conversion. Nevertheless, as long as there are sufficient Na^+ and electron densities, thermospheric Na layers can still form. Therefore, the convergence of ion layers is a necessary condition for the formation of neutral layers, while the temperature serves only to accelerate or decelerate the neutralization process. On this aspect, the existence of vertical shears in horizontal winds is critical to layer formation. Because the tide-induced wind shear is the major mechanism for vertical ion convergence via the $\vec{V} \times \vec{B}$ Lorentz force at low latitudes [e.g., *Carter and Forbes*, 1999], the thermospheric metal layers are governed by the tidal phase as observed at Lijiang and Arecibo.

4. Conclusions

Thermospheric Na layers have been observed unequivocally up to 170 km at Lijiang, China, with ~33% occurrence rate in 2012. Although the Na densities inside the layers are low, about 1–6 cm^{-3} at 130–170 km, all of the layers exhibit a clear downward phase progression with a descending rate of 11–12 km/h, which is consistent with the vertical phase speed of semidiurnal tides. All of the observed layer events correspond to strong to moderate equatorial fountain effects, bolstering our hypothesis that the deposit of metallic ions from the equatorial region to low latitudes via the fountain effect provides the Na^+ ions in the thermosphere over Lijiang. Adopting the theory by *Chu et al*. [2011] and *Yu and Chu* [2014] and the hypothesis by *Tsuda et al*. [2015], we further hypothesize that the thermospheric Na layers are formed through the neutralization of the tidal-wind-shear-converged Na^+ layers via direct recombination $Na^+ + e^- \rightarrow Na + h\nu$. An envelope calculation using reasonable ion and electron densities shows good consistency with the observations.

The Lijiang results nicely complement the observations of thermospheric Fe layers at McMurdo, indicating that thermospheric metal layers are not limited to Fe or the location of McMurdo. Thermospheric metal layers are likely a global phenomenon, providing potential tracers for exploring the neutral properties of the space-atmosphere integration region, especially around altitudes of 100–200 km. Quantitative explanations of the lidar observations would require detailed modeling studies in the future.

Acknowledgments

We sincerely acknowledge Xiaoli Zhang for providing the GSWM-09 data. We are grateful to Zhibin Yu, John A. Smith, Xian Lu, Weichun Fong, and Cao Chen for valuable discussions. The TEC data used in this study were distributed by an IGS data archive center. We also acknowledge the China Research Institute of Radiowave Propagation (CRIRP) for providing the ionosonde data at Kunming. This work was supported by the Projects of the Chinese Academy of Sciences (KJCX2-EW-J01 and KZZD-EW-0101), the National Natural Science Foundation of China (41322029, 41474129, 41121003, 41025016, and 41204108), the National Basic Research Program of China (2012CB825605), and Youth Innovation Promotion Association of the Chinese Academy of Sciences (2011324). Q.G. sincerely acknowledges the scholarship provided by the Chinese Scholarship Council. X.C. was partially supported by the National Science Foundation grants PLR-1246405 and AGS-1136272. The data used in this work are available upon request.

References

Bishop, R. L., and G. D. Earle (2003), Metallic ion transport associated with midlatitude intermediate layer development, *J. Geophys. Res.*, *108*(A1), 1019, doi:10.1029/2002JA009411.

Carter, L. N., and J. M. Forbes (1999), Global transport and localized layering of metallic ions in the upper atmosphere, *Ann. Geophys.*, *17*, 190–209, doi:10.1007/s00585-999-0190-6.

Chu, X., and G. C. Papen (2005), Resonance fluorescence lidar for measurements of the middle and upper atmosphere, in *Laser Remote Sensing*, edited by T. Fujii and T. Fukuchi, pp. 179–432, CRC Press, Taylor and Francis, Boca Raton, Fla.

Chu, X., W. Pan, G. C. Papen, C. S. Gardner, and J. A. Gelbwachs (2002), Fe Boltzmann temperature lidar: Design, error analysis, and initial results at the North and South Poles, *Appl. Opt.*, *41*, 4400–4410.

Chu, X., Z. Yu, C. S. Gardner, C. Chen, and W. Fong (2011), Lidar observations of neutral Fe layers and fast gravity waves in the thermosphere (110–155 km) at McMurdo (77.8°S, 166.7°E), Antarctica, *Geophys. Res. Lett.*, *38*, L23807, doi:10.1029/2011GL050016.

Chu, X., et al. (2013), Lidar observations of thermospheric Fe layers, temperatures and gravity waves at McMurdo, Antarctica, paper presented at Coupling, Energetics and Dynamics of Atmospheric Regions (CEDAR) Workshop, Boulder, Colo., June.

Chu, X., Z. Yu, W. Fong, C. Chen, J. Zhao, I. F. Barry, J. A. Smith, X. Lu, W. Huang, and C. S. Gardner (2015), From Antarctica lidar discoveries to OASIS exploration, paper presented at 27th International Laser Radar Conference, New York City, July.

Collins, S. C., et al. (2002), A study of the role of ion-molecule chemistry in the formation of sporadic sodium layers, *J. Atmos. Sol. Terr. Phys.*, *64*, 845–860.

Cox, R. M., and J. M. C. Plane (1998), An ion-molecule mechanism for the formation of neutral sporadic Na layers, *J. Geophys. Res.*, *103*, 6349–6359, doi:10.1029/97JD03376.

Daire, S. E., J. M. C. Plane, S. D. Gamblin, P. Soldan, E. P. F. Lee, and T. G. Wright (2002), A theoretical study of the ligand-exchange reactions of Na+.X complexes (X = O, O_2, N_2, CO_2 and H_2O): Implications for the upper atmosphere, *J. Atmos. Sol. Terr. Phys.*, *64*, 861–865.

Dou, X. K., S. C. Qiu, X. H. Xue, T. D. Chen, and B. Q. Ning (2013), Sporadic and thermospheric enhanced sodium layers observed by a lidar chain over China, *J. Geophys. Res. Space Physics*, *118*, 6627–6643, doi:10.1002/jgra.50579.

Friedman, J. S., X. Chu, C. G. M. Brum, and X. Lu (2013), Observation of a thermospheric descending layer of neutral K over Arecibo, *J. Atmos. Sol. Terr. Phys.*, *104*, 253–259.

Gelbwachs, J. A. (1994), Iron Boltzmann factor LIDAR: Proposed new remote-sensing technique for mesospheric temperature, *Appl. Opt.*, *33*, 7151–7156.

Hagan, M. E., and J. M. Forbes (2002), Migrating and nonmigrating diurnal tides in the middle and upper atmosphere excited by tropospheric latent heat release, *J. Geophys. Res.*, *107*(D24), 4754, doi:10.1029/2001JD001236.

Hagan, M. E., and J. M. Forbes (2003), Migrating and nonmigrating semidiurnal tides in the middle and upper atmosphere excited by tropospheric latent heat release, *J. Geophys. Res.*, *108*(A2), 1062, doi:10.1029/2002JA009466.

Höffner, J., and J. S. Friedman (2004), Metal layers at high altitudes: A possible connection to meteoroids, *Atmos. Chem. Phys. Discuss.*, *4*, 399–417.

Höffner, J., and J. S. Friedman (2005), The mesospheric metal layer topside: Examples of simultaneous metal observations, *J. Atmos. Sol. Terr. Phys.*, *67*, 1226–1237.

Kopp, E. (1997), On the abundance of metal ions in the lower ionosphere, *J. Geophys. Res.*, *102*, 9667–9674, doi:10.1029/97JA00384.

Lübken, F.-J., J. Höffner, T. P. Viehl, B. Kaifler, and R. J. Morris (2011), First measurements of thermal tides in the summer mesopause region at Antarctic latitudes, *Geophys. Res. Lett.*, *38*, L24806, doi:10.1029/2011GL050045.

Pi, X., A. J. Mannucci, B. A. Iijima, B. D. Wilson, A. Komjathy, T. F. Runge, and V. Akopian (2009), Assimilative modeling of ionospheric disturbances with FORMOSAT-3/COSMIC and ground-based GPS measurements, *Terr. Atmos. Oceanic Sci.*, *20*, 273–285.

Plane, J. M. C. (2003), Atmospheric chemistry of meteoric metals, *Chem. Rev.*, *103*, 4963–4984.

Plane, J. M. C., W. Feng, and E. C. M. Dawkins (2015), The mesosphere and metals: Chemistry and changes, *Chem. Rev.*, doi:10.1021/cr500501m.

Roddy, P. A., G. D. Earle, C. M. Swenson, C. G. Carlson, and T. W. Bullett (2004), Relative concentrations of molecular and metallic ions in midlatitude intermediate and sporadic-E layers, *Geophys. Res. Lett.*, *31*, L19807, doi:10.1029/2004GL020604.

Smith, J. A., and X. Chu (2015), High-efficiency receiver architecture for resonance-fluorescence and Doppler lidars, *Appl. Opt.*, *54*(11), 3173–3184, doi:10.1364/AO.54.003173.

Tsuda, T. T., X. Chu, T. Nakamura, M. K. Ejiri, T. D. Kawahara, A. S. Yukimatu, and K. Hosokawa (2015), A thermospheric Na layer event observed up to 140 km over Syowa Station (69.0°S, 39.6°E) in Antarctica, *Geophys. Res. Lett.*, *42*, 3647–3653, doi:10.1002/2015GL064101.

Verner, D. A., and G. J. Ferland (1996), Atomic data for astrophysics. I. Radiative recombination rates for H-like, He-like, Li-like, and Na-like ions over a broad range of temperature, *Astrophys. J. Suppl.*, *103*(4), 467–473.

Wang, J., Y. Yang, X. Cheng, G. Yang, S. Song, and S. Gong (2012), Double sodium layers observation over Beijing, China, *Geophys. Res. Lett.*, *39*, L15801, doi:10.1029/2012GL052134.

Wei, K., et al. (2010), First light on the 127-element adaptive optical system for 1.8-m telescope, *Chin. Opt. Lett.*, *8*(11), 1019–1021, doi:10.3788/COL20100811.1019.

Whitehead, J. D. (1961), The formation of the sporadic-E Layer in the temperate zones, *J. Atmos. Terr. Phys.*, *20*, 49.

Xue, X. H., X. K. Dou, J. Lei, J. S. Chen, Z. H. Ding, T. Li, Q. Gao, W. W. Tang, X. W. Cheng, and K. Wei (2013), Lower thermospheric-enhanced sodium layers observed at low latitude and possible formation: Case studied, *J. Geophys. Res. Space Physics*, *118*, 2409–2418, doi:10.1002/jgra.50200.

Yu, Z. (2014), Lidar observations and numerical modeling studies of thermospheric metal layers and solar effects on mesospheric Fe layers, PhD dissertation, Univ. of Colo., Boulder.

Yu, Z., and X. Chu (2014), Roles played by electric field, vertical wind and aurora in the source, formation and evolution of thermospheric Fe/Fe+ layers at high latitudes, Abstract presented at 2014 Fall Meeting, AGU, San Francisco, Calif., Dec.

Zhang, X., J. M. Forbes, and M. E. Hagan (2010a), Longitudinal variation of tides in the MLT region: 1. Tides driven by tropospheric net radiative heating, *J. Geophys. Res.*, *115*, A06316, doi:10.1029/2009JA014897.

Zhang, X., J. M. Forbes, and M. E. Hagan (2010b), Longitudinal variation of tides in the MLT region: 2. Relative effects of solar radiative and latent heating, *J. Geophys. Res.*, *115*, A06317, doi:10.1029/2009JA014898.